Available online at www.sciencedirect.com
ScienceDirect
Spectrochimica Acta Part A 69 (2008) 971–979
SPECTROCHIMICA ACTA PART A
www.elsevier.com/locate/saa

Synthesis and spectral properties of some bis-substituted formazans

Habibe Tezcan *

Department of Chemistry, Gazi University, Faculty of Gazi Education, Teknikokullar, 06500 Ankara, Turkey

Received 8 February 2007; received in revised form 24 May 2007; accepted 26 May 2007

Abstract

Novel, 1,4-bis-[3,3′-phenyl-5,5′-(*o*-carboxyphenyl)-formaz-1-yl]-benzene-*o*-sulphonic acid and its derivatives contained –OH group at the *o*-, *m*-, *p*-positions of the 3-phenyl ring were synthesized. The structures of the formazans were confirmed by elemental analyses, GC-mass, IR, ^{1}H NMR, UV–vis spectra. Their absorption properties were investigated. It was seen that λ_{max} values shifted towards shorter wave lengths by 130 nm in CSPF relative to 1,3,5-triphenylformazan (TPF) due to the fact that the structure of CSPF contained electron withdrawing –COOH and $-SO_3H$ groups (hypsochromic effect). With binding of –OH group to 3-phenyl ring of CSPF, it was observed a small bathochromic effect in accordance to the electron donating effect of –OH group.

Keywords: Bis-substituted formazans dyes; Spectroscopy; IR spectroscopy; Mass spectra; Substituent effect

1. Introduction

There are numerous studies related to formazans such as their synthesis, structural properties, photochromic transitions, tautomer formation, redox potentials [1–6] and synthesis of crown formazans [7,8]. Metal–formazan complexes were synthesized and their thermogravimetric analyses, dissociation and stability constants, formation constants and electrochemical behaviors were examined [9–12].

The IR and Raman spectra were determined [5,13] and the substituents effect upon complex forming, pK_a values and the dependence of their absorption properties upon pH were determined [14–16].

Formazan/tetrazolium system is described as the marker of vitality [17]. These compounds are used in Brucella-ring test in milk [18]. Blue tetrazolium/formazan systems are used to demonstrate enzymes activity in normal and neoplastic tissues but it was found to be 10 times more toxic in vivo (mice) than mono tetrazolium/formazan system itself [19]. Formazan/tetrazolium system is quite useful in the determination of the effect and the selection of anti-cancer drugs [20,21]. However, Kebler and Furusaki states that they cannot act as a marker every time, since the age of the cell and medium are also important [22]. Additional, substituents effects on formazans were investigated [23–25].

Formazans are easily oxidized to give tetrazolium salts. When given to a living organism these salts are reduced back to formazan depending upon the viability of the organism. These enables the viability of the organism be tested by monitoring formazan formation with spectroscopy. That is why the spectroscopic investigation of formazans is of importance.

The purpose of this study is to synthesize water-soluble macromolecular bis-formazans with various structures and to investigate their spectral properties. Also it is hoped that the formazans synthesized in this study are less toxic and more suitable for medical applications.

Formazans are colored compound ranging from red to orange or blue depending upon their structures. However, they did not have their deserved place in dying industry as seen the application of these compounds is based upon their color features. That is why this study is mainly focused on λ_{max} values of various formazans and the substituents which effect the λ_{max} values.

Formazans are polydentate ligands with donor atoms and they are used for analytical purposes for forming complexes with trace metals. It also hoped that the formazans synthesized in this study are suitable for these applications.

2. Results and discussion

This study was carried out in three stages. The first step, TPF (**1**) (Scheme 1a) and new substituted bis-formazans (**2**–**5**)

* Fax: +90 312 2228483.
E-mail address: habibe@gazi.edu.tr.

1386-1425/$ – see front matter © 2007 Elsevier B.V. All rights reserved.
doi:10.1016/j.saa.2007.05.061

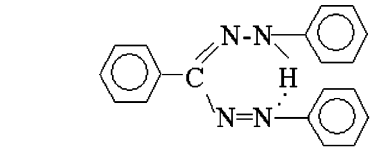

1-a

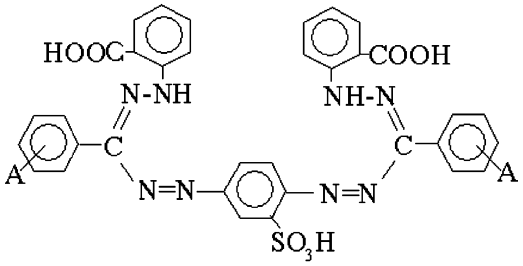

1-b

Comp.	A	Abbrev.
1	--	TPF
2	H	CSPF
3	*o*-OH	*o*-HCSPF
4	*m*-OH	*m*-HCSPF
5	*p*-OH	*p*-HCSPF

Scheme 1. The structure of the formazans synthesized.

(Scheme 1b) were synthesized; in the second step, spectral properties of these formazans were determined. In the third stage their structures and λ_{max} values were elucidated. The shifts in λ_{max} values of **2**–**5** were evaluated in comparison to TPF (**1**) and the shifts in λ_{max} values of compounds (**3**–**5**) were evaluated in comparison to CSPF (**2**).

2.1. Synthesis of formazans

There are three distinctive routes proposed for the synthesis of formazans in literature [6]. The first one is the condensation of aromatic and aliphatic aldehydes with phenyl hydrazine and the coupling reaction of the resulting hydrazones with diazonium salts [6]. Although this is highly cumbersome and resulting products are difficult to purify, it has the advantage of be able to synthesizing symmetrical and asymmetrical formazans [6,24]. The second way is the coupling of active methylene compounds with two mols diazonium cations. This is highly practical and easy but only gives symmetrical formazans [6,13]. The third way is the phase transfer. However, it requires special regents such as crown ethers and tetrabuthyl ammonium bromide, etc. [6].

The formazans in this study were synthesized by the first way, coupling of hydrazones with diazonium cations in basic media at −5 to 0 °C. The necessary hydrazones were obtained by the condensation reaction of benzaldehyde (or substituted benzaldehydes) and phenylhydrazine (or substituted phenylhydrazine) at pH 5–6. This is the most difficult and low yielding route in the synthesis of formazans. The purification of the products is cumbersome and requires patience [6,25]. The reason for the preference of this way in spite of all these setbacks is that the starting material is easily available in every laboratory. We tried to increase the yield in order to provide a cheap way to synthesize formazans for medical, dying and analytic applications.

Mechanism of TPF formation was traced with UV–vis spectra. The fact that NH proton is more acidic than CH proton, the first diazonium coupling was realized through NH proton, forming orange colored 4-benzylidene-1,3-diphenyltetraz-1-en. This is highly instable in basic media and gave an intermolecular rotation turning into red colored formazans. This is in accordance with previous study [25].

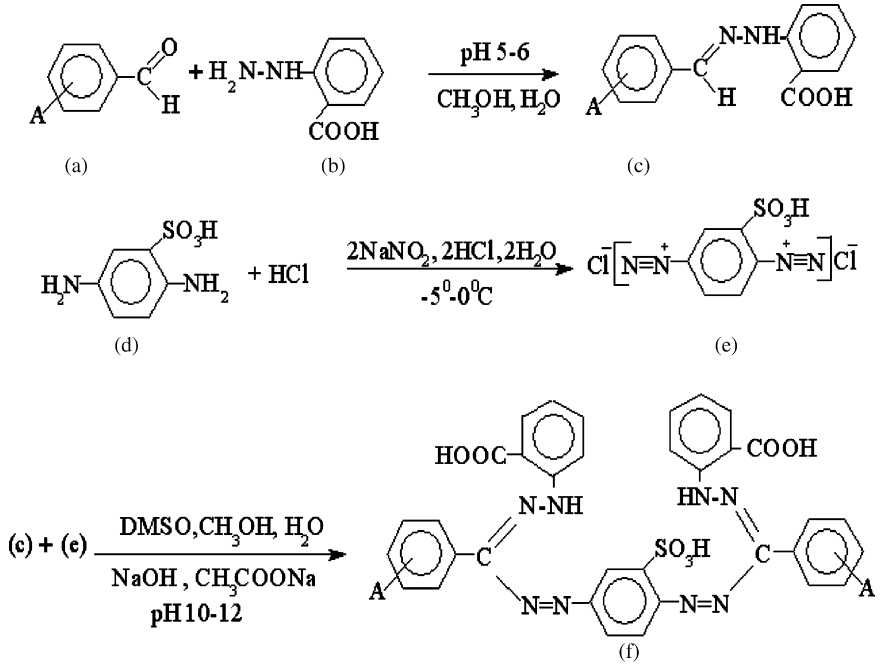

Scheme 2. Synthesis of formazans.

Table 1
Experimental data and elemental analysis of the formazans synthesized

Comp.	mp (°C) (lit.)	Yield (%) (lit.)	Color	Elemental analysis							
				Calculated				Found			
				C	H	N	S	C	H	N	S
1	172–173 (172–174)[6]	75 (54)[6],(63)[24]	Cherry red	76.00	5.33	18.66	–	75.97	5.29	18.69	–
2	255–256	55	Salmon	59.13	3.76	16.23	4.63	59.01	3.67	16.12	4.68
3	213	46	Cyclamen	56.51	3.60	15.51	4.43	56.48	3.54	15.47	4.55
4	>300	53	Yellow-brown	56.51	3.60	15.51	4.43	56.48	3.54	15.47	4.55
5	207	54	Light brown	56.51	3.60	15.51	4.43	56.48	3.54	15.47	4.55

The basic buffer solutions employed were 0.1 M $HClO_4$ + 0.05 M borax solution (pH 7.60–9.00) and 0.1 M NaOH + 0.05 M borax solution (pH 9.30–10.80). However, the best yield was obtained with the NaOH + CH_3COONa buffer solution (pH 10–12). The reaction scheme is provided in Scheme 2 and the experimental data were tabulated in Table 1. The structures of the formazans were elucidated by elemental analysis, Mass, IR, ^{1}H NMR, UV–vis, spectral data.

As seen from Table 1 that the yield of TPF is higher than that reported in literature [6,24]. The lowest yield was obtained at the *o*-position in **2**–**5** formazans. This can be attributed to the fact that substituents are the closest to the reaction site in this position, which sterically hinders the coupling reaction. The relative increase in yield at both *m*- and *p*-positions verifies this hypothesis. If an electronic effect (resonance and inductive effects) were dominant, the best yield would be obtained at the *o*-position. The biggest difficulty was encountered in the synthesis of *m*-OH bis-formazan **4**. The resulting product was resinous and non-crystallizable. The synthesis was repeated several times using dilute conditions and various pH values, to prevent this situation. However, it was not possible to obtain perfect crystals.

2.2. ^{1}H NMR spectra

As seen from Table 2 the ^{1}H NMR data shows the δ values of CSPF (**2**) shifted to lower field compared to those of TPF. For instance δ a value for Ar–H is 7.55 ppm in TPF (**1**) and shifted to the lower field (8.55 ppm) in CSPF (**2**). This is perfectly justifiable since there are electron withdrawing groups such as two –COOH and one $-SO_3H$ in the structure of CSPF (**2**). In compounds **3**–**5** the substitution of –OH group at the *o*-, *m*-, *p*-positions resulted δ values to show a slight shift to higher fields compared with compound **2**. This is quite expectable from the electron donating feature of –OH group. However, the shift towards the higher fields as a result of substituting OH groups to the ring is lower compared with the shift towards the lower fields as a result of substitution of –COOH and $-SO_3H$. For instance δ value makes a shift of 0.63 ppm higher field from CSPF to *o*-HCSPF (8.55–7.92 ppm). This $\Delta\delta$ value is lower at the *m*-position compared with *o*-position since there is no resonance effect and only a weak inductive effect at the *m*-position. This shift at the *p*-position is higher than *m*- and lower than *o*-positions. Because at the *p*-position the inductive effect is diminished but there is a resonance effect. That is why the δ values of compounds **3**–**5** are at highly lower fields compared with that of TPF but a little bit higher than CSPF. These peaks are compatible with the structure depicted in Fig. 1 [26]. The N–H, Ar–OH, –COOH and $-SO_3H$ groups were observed in the expected regions (Table 2). Fig. 1 shows the ^{1}H NMR spectra of CSPF, *o*-HCSPF, *p*-HCSPF in $CDCl_3$ at 25 °C.

2.3. IR spectra

The IR data reported in Table 3 reveals that for TPF, the –C=N stretching band is located at 1500 cm^{-1}. This shows the presence of chelation through intramolecular hydrogen bonding in TPF. The formation of a hydrogen bond between the electron pair on –N=N– and the hydrogen of NH turns the molecule into chelate and causes intramolecular proton transfer [1,5,25]. There is an element of symmetry in the molecule (Scheme 3).

The C=N stretching peaks are observed at 1635–1520 cm^{-1} in compounds **2**–**5**. This due to the fact that bis-formazans are containing $-SO_3H$ group and two –COOH groups which increase the steric hindrance and therefore decreasing chelation strength. However, it is observed that although in a very small extend there is the presence of chelate form in the equilibrium. If C=N stretching band is located at 1565–1551 cm^{-1} or higher, there is no chelation and the molecule is in the excited

Table 2
The ^{1}H NMR data of formazans (**1**–**5**) (400 MHz, in $CDCl_3$)

Comp.	Ar—H	N—H	Ar—OH	COOH	SO_3H
1	7.55–6.70(m,15H)	1.14 (s,1H)	–	–	–
2	8.55–6.90(m,21H)	2.50–2.25(s,2H)	–	10.90(s,2H)	11.28(s,1H)
3	7.92–6.85(m,19H)	2.75–2.60(s,2H)	3.10(s,2H)	10.80(s,2H)	11.27(s, 1H)
4	8.50–6.65(m,19H)	2.55–2.20(s,2H)	3.40(s,2H)	10.85(s,2H)	10.85(s,1H)
5	7.98–6.65(m,19H)	2.05–1.70(s,2H)	3.20(s,2H)	10.85(s,2H)	10.85(s,1H)

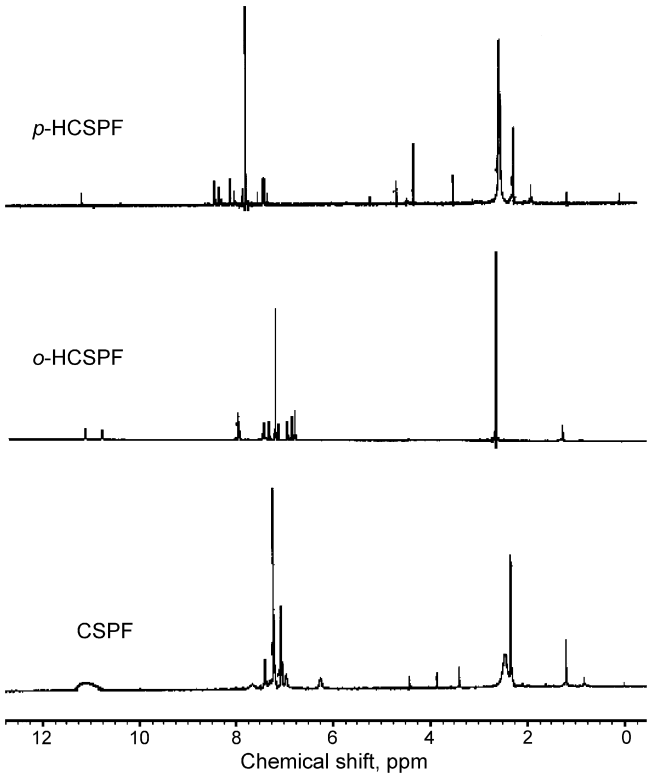

Fig. 1. ^{1}H NMR spectra of CSPF, *o*-HCSPF, *p*-HCSPF measured in $CDCl_3$ at 25 °C.

state. On the other hand, the location of the C=N stretching band between 1510 and 1500 cm^{-1} is the indication of chelation [6,27]. Our upper limit for formazans (**2**–**5**) at 1635 cm^{-1} is the indication of the absence of chelation while the lower limit of 1520 cm^{-1} verifies the presence of a very small chelation. The fact that the peaks at 1530 cm^{-1} are very weak is also another indication of the very small extent of the chelation strength.

–N=N– stretching bands in TPF was observed 1358 cm^{-1}. This value shows chelating in the molecule since this band is expected at 1450–1400 cm^{-1}. This decrease in wave number stems from the resonance stabilization due to the formation of chelation in the molecule. In substituted formazans (**2**–**5**), –N=N– stretching bands was observed between 1455 and 1330 cm^{-1}. These values reveal that the excited state of the molecule, distortion of the chelation and probable the presence of trans-formation (1455 cm^{-1}). The values of 1420 cm^{-1} or higher is the indication of –N=N– bands of the formazans without chelation and the values of 1442 cm^{-1} or higher is the verification of the trans conformation of the molecule [6,27]. Also the very weak bands observed between 1360 and 1335 cm^{-1} is the proof of the presence of chelate form in equilibrium with a very small extend. CNNC skeleton vibration peaks were observed in the fingerprint region as expected from the structure of formazans. N–H and Ar–OH stretching peaks appeared between 3600 and 3000 cm^{-1}. Other peaks were also in accordance with structure of formazans. These results confirm the formula giving in Scheme 1. The IR spectra of TPF, CSPF, *o*-, *m*-, *p*-HCSPF are shown in Fig. 2(A–E).

2.4. Mass spectra

The mass spectra of formazans (**1**–**5**) were recorded and their molecular ion peaks confirm the suggested formula Scheme 1. The calculated and found values of the molecular weights of some of the formazans are given in Section 3. Representative mass spectrum of the formazan (*p*-HCSPF, **5**) is shown in Fig. 3. The spectrum shows numerous peaks representing successive degradation of the molecule. The observed peak at *m*/*z* 722.01 (Calcd. 722.15) represents the molecular ion peak of the complex with 3.27% abundance. Scheme 4 demonstrates the proposed paths of the decomposition steps for the investigated formazan (**5**). One of the strongest peaks (base peak) at *m*/*z* 212.35 represents the stable species $C_6H_4O_3N_4S$. Elemental analysis and mass spectroscopic data also corroborated the structures proposed in Scheme 1.

Table 3
The IR spectral data of formazans (**1**–**5**) (in KBr, cm^{-1})

Comp.	C=N stretching	N=N stretching	Aromatic C=C stretching	CNNC Skeletal vibration	NH + Ar—OH stretching	—COOH stretching	—SO_3H stretching
1	1500	1358	1600	800–600	3050–3000	–	–
2	1540–1580	1455–1335	1629	930–600	3600	3400–3300	1420–1330
3	1590–1520	1418–1330	1620	850–620	3480–3300	3390–3300	1385–1220
4	1635–1580	1450–1335	1630	920–610	3600–3200	3420–3210	1410–1340
5	1600–1530	1420–1335	1622	850–620	3400–3220	3395–3300	1380–1220

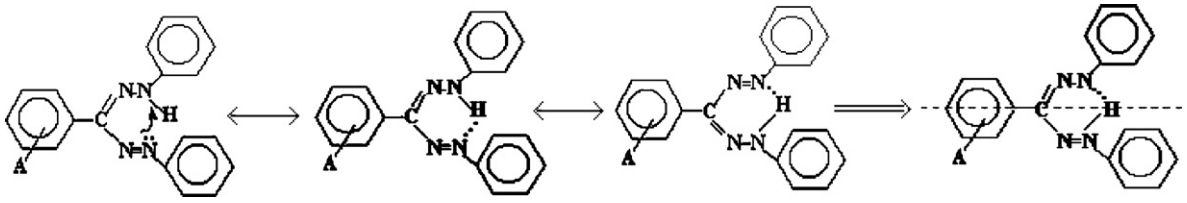

Scheme 3. Molecular chelating and symmetry.

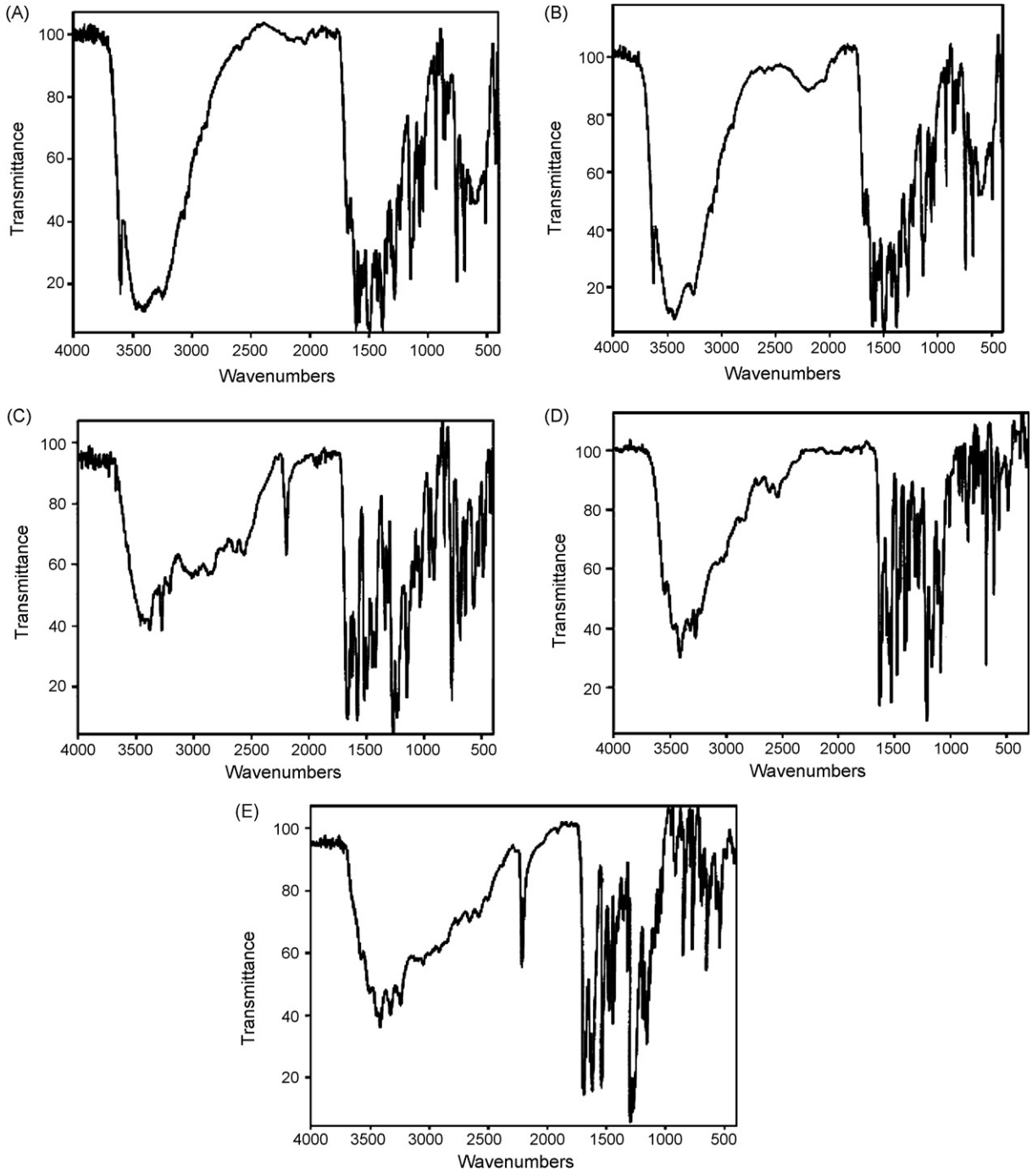

Fig. 2. IR spectra of: (A) TPF; (B) CSPF; (C) *o*-HCSPF; (D) *m*-HCSPF; (E) *p*-HCSPF.

2.5. Absorption spectra

There are three distinctive peaks in the UV–vis spectra of formazans. The λ_{max1} values are specific to formazans skeleton. This is why that this study is concerned with λ_{max1} values. Formazan peaks λ_{max1} values are generally observed at 410–500 nm and may be shifted to 350–600 nm depending upon the structure. These peaks are due to $\pi \rightarrow \pi^*$ and $n \rightarrow \pi^*$ electronic transitions in formazan skeleton. λ_{max2} Values generally appeared at 300–350 nm, corresponding to electronic transitions of –N=N– group in the molecule. λ_{max3} Values sometimes observed at 270–300 nm originate from $n \rightarrow \pi^*$ transitions of –C=N– groups in the molecule [3,24].

The electronic absorption spectra of formazans were recorded in methanol, DMSO, DMF, 1,4-Dioxane, CH_2Cl_2. As a sample UV–vis value of in methanol was interpreted and tabulated in Table 4. The λ_{max1} values are observed for TPF (**1**) and bis-formazan CSPF (**2**) at 483 and 352 nm, respectively. There is a shift of $\Delta\lambda_{max1} = 131$ nm towards shorter wavelengths (hypsochromic effect). This is in accordance with the fact that CSPF contains compared with TPF electron withdrawing groups such as –COOH and $-SO_3H$ in its structure (Scheme 1b). In com-

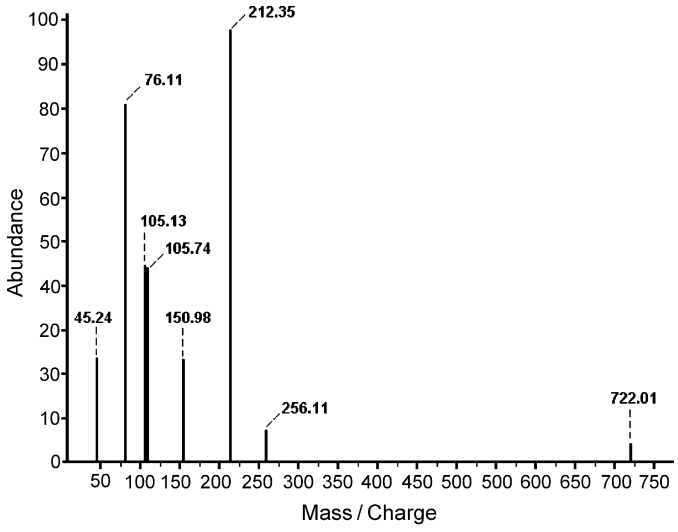

Fig. 3. Mass spectrum of the formazan (*p*-HCSPF, **5**).

pounds **3**–**5** there are OH groups attached to 3,3-phenyl rings in addition to electron withdrawing, such as –COOH and $-SO_3H$ groups in compound **2**. The λ_{max1} values were observed at 356, 353 and 354 nm as a result of the attachment of OH groups to *o*-, *m*-, *p*-positions of 3,3′-phenyl rings (compounds **3**–**5**). This is explained by the electron donating nature of OH group. The most distinctive shift was observed at the *o*-position ($\Delta\lambda_{max1} = 4$). There is resonance effect as dominate. That is because OH group attached at the *o*-position is the closest to the reaction site. There is no resonance effect at the *m*-position and the inductive effect is highly diminished. That was why there was a small shift such as $\Delta\lambda_{max1} = 1$ nm in this position. At the *p*-position the inductive effect vanishes and –OH acts as an only electron donating group with resonance effect. Since it is far away from the reaction site compared with *o*-position, the shift of *p*-position is lower than *o*-position but higher than *m*-position where there is no resonance effect ($\Delta\lambda_{max1} = 2$ nm).

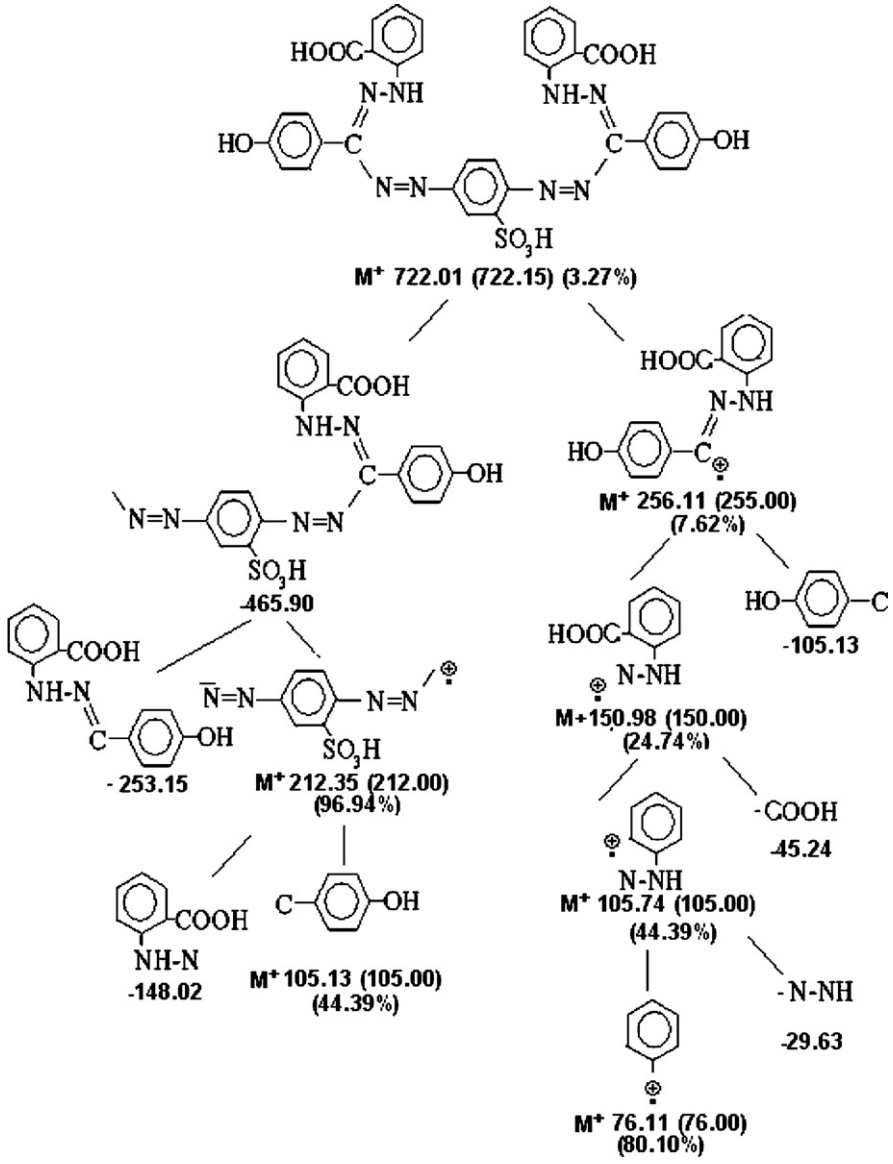

Scheme 4. Proposed fragmentation pattern of *p*-HCSPF (**5**).

Table 4
UV–vis absorption λ_{max} values of formazans (**1–5**) (CH_3OH, 10^{-4} moll^{-1})

Comp.	λ_{max1} (nm) (Abs)	λ_{max2} (nm) (Abs)	$\Delta\lambda_{max1}$ according to TPF (nm)	$\Delta\lambda_{max1}$ according to CSPF (nm)
1	483 (0.370)	335 (0.614)	–	–
2	352 (0.912)	233 (0.565)	131	–
3	356 (1.590)	218 (1.714)	127	4
4	353 (0.912)	218 (1.714)	130	1
5	354 (1.222)	219 (1.282)	129	2

Column 4: $\Delta\lambda_{max1} = \lambda_{max1}$ (TPF) − λ_{max1} (substituted formazans). Column 5: $\Delta\lambda_{max1} = \lambda_{max1}$ (CSPF) − λ_{max1} (HCSPF).

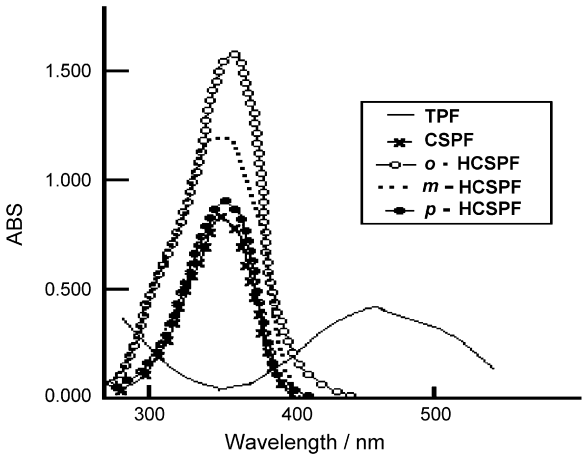

Fig. 4. The electronic absorption of formazans in CH_3OH, 10^{-4} mol/l.

Another important point was the λ_{max1} values of bis-formazans (**2–5**) relative to TPF (**1**). λ_{max1} Values of compounds **2–5** were observed at 352, 356, 353, 354 nm, respectively. There was a shift towards a relatively short wavelength (hypsochromic effect) due to the fact that bis-formazans contain highly electron withdrawing groups. The fact that there were shifts of 131,127, 130, 129 nm for substituted bis-formazans **2–5** relative to TPF is in good accordance with the structure of these compounds (Scheme 1). These shifts changed slightly to the opposite direction upon attachment of –OH groups to the molecule. Fig. 4 shows the electronic absorption spectra of formazans in CH_3OH.

UV–vis absorption λ_{max1} values of formazans were tabulated in Table 5 and given in Fig. 5A–D. As seen λ_{max1} values were changed with solvent species.

3. Experimental

All chemicals were obtained from Merck and Fluka expect sodium hydroxide that was purchased from Sigma–Aldrich. All chemicals and solvents used in the syntheses were of reagent grade and were used without further purification.

3.1. Synthesis of 1,3,5-triphenylformazan (*TPF, 1*)

1,3,5-Triphenylformazan was synthesized by the reaction of benzaldehyde (1.06 g, 0.01 mol), phenylhydrazine (1.08 g, 0.01 mol), aniline (0.93 g, 0.01 mol), concentrated HCl (5 ml) and sodium nitrite (0.75 g) in a methanol, at 0–5 °C described in literature [24,25].

3.2. Synthesis of 1,4-bis-[3,3′-phenyl-5,5′-(o-carboxyphenyl)-formaz-1-yl]-benzen-2-sulphonic acid (CSPF, 2) and;1,4-bis-[3,3′-(o-, m-, p-hydroxyphenyl)-5,5′-(o-carboxyphenyl)-formaz-1-yl]-benzen-2-sulphonic acid (o-, m-, p- HCSPF, *3–5*)

Benzaldehyde and *o*-, *m*-, *p*-hydroxybenzaldehyde (0.02 mol) were dissolved with methanol (40 ml). *o*-Hydrazynobenzoic acid (0.02 mol) was dissolved in methanol (80 ml) and water (20 ml). *o*-Hydrazynobenzoic acid solution was added to the benzaldehyde and *o*-, *m*-, *p*-hydroxybenzaldehyde solutions with constant stirring in dropwise fashion adjusting the pH 5–6.

Yellow colored hydrazone of **2**, light yellow colored hydrazone of **3**, yellow colored hydrazone of **4** and dark yellow colored hydrazone of **5** compounds were precipitated out. The products are recrystallized from methanol–water mixture. Hydrazones were dissolved in methanol (75 ml) and water (25 ml) under reflux. The basic buffer solution was prepared by adding NaOH (2.50 g) and sodium acetate (3.50 g) to 200 ml methanol under reflux and added to hydrazone solutions as prepared above. The mixture was cooled down to 0 °C and kept ready for the coupling reaction (stock solution).

At the other side a *o*-sulphobenzen-1,4-di-diazonium chloride solutions were prepared with 2,5-diaminobenzen sulphonic acid (1.88 g, 0.01 mol) concentrated HCl (5 ml), $NaNO_2$

Table 5
UV-vis absorption λ_{max} values of formazans at different solvents (**1–3**, **5**)

Solvents					
Comp.	CH_3OH λ_{max1} (nm) (Abs)	DMSO λ_{max1} (nm) (Abs)	DMF λ_{max1} (nm) (Abs)	1,4-Dioxane λ_{max1} (nm) (Abs)	CH_2Cl_2 λ_{max1} (nm) (Abs)
1	483 (0.370)	487 (0.522)	484 (0.757)	486 (0.276)	484 (0.853)
2	352 (0.912)	364 (0.673)	363 (1.292)	358 (1.562)	357 (0.789)
3	356 (1.590)	359 (1.111)	356 (0.494)	364 (0.912)	367 (0.524)
5	354 (1.222)	362 (1.878)	362 (1.849)	363 (0.532)	367 (1.749)

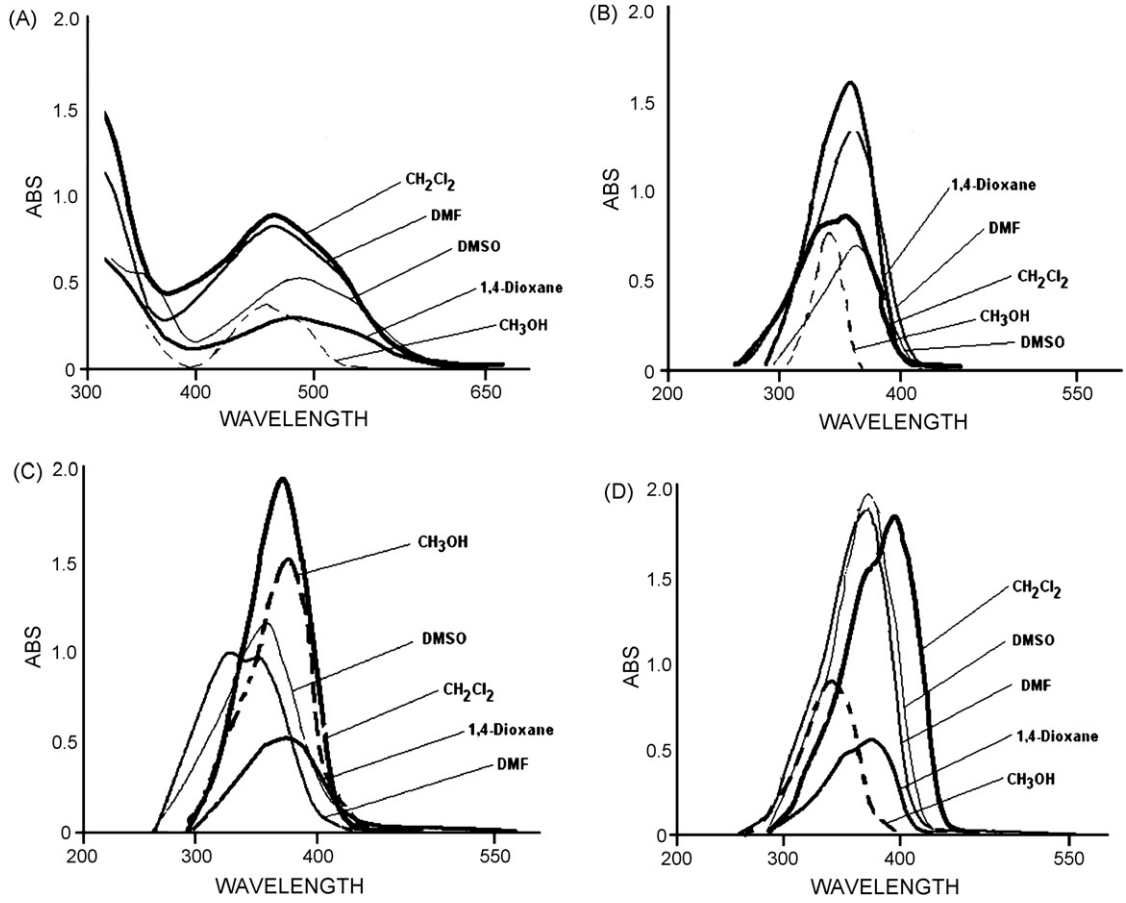

Fig. 5. The electronic absorption in CH_3OH, DMSO, DMF, 1,4-Dioxane, $CH_2Cl_2 \cdot 10^{-4}$ mol/l: (A) compound **1**; (B) **2**; (C) **3**; (D) **5**.

(1.40 g,0.02 mol) in usual way at −5 to 0 °C. This diazonium solution was added in dropwise manner to basic buffer hydrazone solutions as prepared above and cooled down to 0 °C, in ice bath at constant stirring for the coupling reaction. Care was taken for the temperature not exceeds −5 to 0 °C. The reaction was completed in about 120–150 min. The mixture was stirred for 2–3 more hours at the same temperature. The mixture was kept in the fridge at the same temperature for 3–5 days. The salmon colored (**2**), cyclamen colored (**3**), brown colored (**4**) red-brown colored (**5**) formazans precipitated out. The product was recrystallized from methanol + water + dioxan mixture.

Mass analysis for $C_{34}H_{26}O_7N_8S$, M: 690.30. Mass *m*/*z* (eV): 690.12 (M+, 0.51%), 658 (2.21%), 599 (5.27%), 520 (11.48%), 300 (47.25%), 255 (78.89%), 240 (67.33%), 188 (22.46%).

Mass analysis for $C_{34}H_{26}O_9N_8S$, M: 722.15. Mass: *m*/*z* (eV): 722.01 (M+, 3.27%), 256.11 (7.62%), 212.35 (96.94%), 150.98 (24.74%), 105.74 (44.39%), 76.11 (80.10%), 45.24 (23.60%).

3.3. Physical measurements

^{1}H NMR spectra were recorded on a BRUKER 400 MHz spectrophotometer using $CDCl_3$, in 10^{-4} M. The IR spectra were recorded on a MATTSON 100-FT-IR spectrophotometer between 4000 and 400 cm^{-1} using KBr pellets. The UV–vis spectra were obtained with UNICAM UV2-100 UV–vis spectrophotometer using 1 cm quartz cell, in 10^{-4} M CH_3OH, DMSO, DMF, 1,4-Dioxane and CH_2Cl_2 using 325 nm lamp. The elemental analysis studies were carried out by LECO-CHNS-932 elemental analyzer. Mass spectra were recorded on a micro mass UK Platform-II device at 70 eV electron impact modes.

Acknowledgement

We are very grateful to the Gazi University Research Fund for providing financial support for this project (Project No: 04/97-09 Ankara-Turkey).

References

[1] L. Hunter, C.B. Roberts, J. Chem. Soc. 9 (1941) 820.
[2] A.M. Mattson, C.O. Jensen, R.A. Dutcher, J. Am. Chem. Soc. 70 (1948) 1284.
[3] G. Arnold, V.C. Schiele, Spectrochim. Acta 25 (1966) 685.
[4] V.C. Schiele, Chemische Berichte 30 (1964) 308.
[5] J.W. Lewis, C. Sandorfy, Can. J. Chem. 61 (1983) 809.
[6] A.R. Katritzky, S.A. Belyakov, D. Cheng, H.D. Durst, Synthesis 5 (1995) 577.
[7] Y.A. Ibrahim, A.H.M. Elwahy, A.H.M. Abbas, Tetrahedron 50 (1994) 11489.
[8] A.A. Abbas, Tetrahedron 54 (1998) 12421.
[9] O.E. Sherif, Y.M. Issa, M.E.M. Hassouna, S.M. Abbas, Monatshefte für Chemie 124 (1993) 627.
[10] A. Uchiumi, A. Takatsu, H. Tanaka, Anal. Sci. 7 (1991) 459.

[11] S.S. Badawy, Y.M. Issa, H.M. Abdel Fattah, Transition Met. Chem. 14 (1989) 401.
[12] G.M. Abou-Elenien, J. Electroanal. Chem. 375 (1994) 301.
[13] U. Yuksel, Post Doctoral Thesis, Turkish Aegean University, 1981.
[14] M. Grote, U. Hüppe, A. Kettrup, Hydrometallurgy 19 (1987) 51.
[15] A. Uchiumi, A. Kawase, Anal. Sci. 7 (1991) 119.
[16] Y.M. Issa, N.T. Abdel Ghani, O.E. Sherif, Bull. Soc. Chim. Fr. 128 (1991) 627.
[17] A.M. Mattson, C.O. Jensen, R.A. Dutcher, Science 5 (1947) 294.
[18] R.M. Wood, Science 112 (1950) 86.
[19] A.M. Rutenberg, R. Gofstein, A.M. Seligman, Cancer Res. 10 (1950) 113.
[20] J.A. Plumb, R. Milroy, S.B. Kaye, Cancer Res. 49 (1989) 4435.
[21] H. Wan, R. Williams, P. Doherty, D.F. Williams, J. Mater. Sci.: Mater. Med. 5 (1994) 154.
[22] M. Kebler, S. Furusaki, J. Chem. Eng. Jpn. 30 (1997) 718.
[23] H. Tezcan, T. Uyar, R. Tezcan, Turk. J. Spectrosc. Aegean Univ. 9 (1988) 8;
H. Tezcan, T. Uyar, R. Tezcan, Turk. J. Spectrosc. Aegean Univ. 10 (1989) 82.
[24] H. Tezcan, S. Can, R. Tezcan, Dyes Pigments 52 (2002) 121.
[25] H. Tezcan, N. Ozkan, Dyes Pigments 56 (2003) 159.
[26] F. Schiman, Nuclear Magnetic Resonance of Complex Molecules, vol. 1, Vieweg and Sohn GmbH, Braunschweig, 1970.
[27] L.J. Bellamy, The Infrared Spectra of Complex Molecules, Methuen, London, 1962.